Construction of new surface air specific humidity data set with high accuracy using multi-satellite data

Tsutomu Hihara, Daishi Satoh and Masahisa Kubota
School of Marine Science and Technology, Tokai University
e-mail : tsutomu@mercury.oi.u-tokai.ac.jp, Address: 3-20-1 Orido, Shimizu, Shizuoka, 424-8610 Japan

1. Introduction

In case of estimating the air-sea turbulent flux such as latent heat flux (LHF), sensible heat flux and momentum flux, a bulk method has been often employed. In a bulk method various fluxes are estimated by substituting various physical quantities into a bulk formula. Generally, a bulk formula estimating LHF is given by

$$LHF = \rho L C_{Ed} U (Q_s - Q_a)$$

where U and Qa is wind speed and surface air specific humidity at a reference height within the atmospheric surface layer, Qs is saturation specific humidity at the sea surface temperature (SST), ρ is air density, L is the latent heat of vaporization and CEd is bulk transfer coefficient. Therefore, we need U, SST and Qa in order to estimate LHF using a bulk method.

Iwasaki et al. (2010) investigated that which error included in the physical quantity largely contributes to the error of LHF in Japanese Ocean Flux Data sets with Use of Remote Sensing Observations 2 (J-OFURO2) (Kubota and Tomita, 2007) product and demonstrated the error of Qa has the largest impact on the error of LHF. Therefore, it is considered that improvement of the Qa estimation leads to estimate precise estimation of LHF.

Our objective in this study is to make the highly accurate Qa and LHF products using the three kinds of satellite sensors; Defense Meteorological Satellite Program (DMSP)/Special Sensor Microwave Imager (SSMI), Aqua/Advanced Microwave Scanning Radiometer for EOS (AMSR-E) and Tropical Rainfall Measurement Mission (TRMM)/TRMM Microwave Imager (TMI).

2. Data

In this study we used in situ data observed by Kuroshio Extension Observatory (KEO) buoy, Tropical Atmosphere Ocean project (TAO) buoy, Triangle Trans-Ocean buoy Network (TRITON) buoy, Prediction and Research Moored Array in the Atlantic (PIRATA) buoy, Research moored array for African-asian-australian Monsoon Analysis and prediction (RAMA) buoy and National Data Buoy Center (NDBC) buoy. The location of each buoy is shown in Figure 1. We use these data observed from 2003 to 2005. Since the highest time resolution for each buoy is 10 minutes or 1 hour, we average 10 minutes data into 1 hour data to unity the time resolution. The red points in Figure 1 show the positions of the buoys which we used for analyses of Figures 3 and 4. For these analyses, we used the data observed by these buoys during one year. Table 1 describes the detailed information about these buoys.

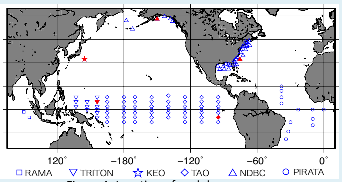

Figure 1. Location of each buoy.

Table 1. Detail information of buoys using in error analysis.

Category	Buoy	Location	Period
(a) Low Latitude (ITCZ)	TRITON	5°N 156°E	2004.1～2004.12
(a') Low Latitude (Non-ITCZ)	TAO	5°S 95°W	2005.1～2005.12
(b) Middle Latitude (Kuroshio)	KEO	32°N 145°E	2004.7～2005.8
(b') Middle Latitude (Gulf)	NDBC	32°N 75°W	2003.1～2003.12
(c) High Latitude	NDBC	58°N 150°W	2005.1～2005.12

Table 2. Observation time of each satellite.

Satellite	Sensor	Equatorial crossing time	
		Ascending	Descending
DMSP F13	SSM/I	18:20	6:20
DMSP F14	SSM/I	20:10	8:10
DMSP F15	SSM/I	21:30	8:30
Aqua	AMSR-E	13:30	1:30
TRMM	TMI	Variable	

We used brightness temperature data observed by five satellite sensors; DMSP/SSMI F13, F14 and F15, Aqua/AMSR-E, TRMM/TMI.

Table 2 shows the equatorial crossing time in local time for each satellite. Because DMSP and Aqua are sun-synchronous polar-orbit satellites, the equatorial crossing time for these satellites is the same everywhere. On the other hand, because TRMM is a non-sun-synchronous satellite, the observation time is variable. Additionally, it should be noted that TRMM observes the region between 40°S and 40°N.

3. Results

(1) Error analysis of daily-averaged surface air specific humidity

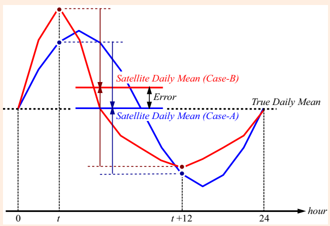

Figure 2. The conception of sampling errors of the data observed every twelve hours.

Generally, surface meteorological variables vary within a day. Therefore, it is considered that a daily-mean value strongly depends on observation time if we estimate it using satellite data. For example, if the variable is periodic and symmetrical within a day such as Case-A in Figure 2, data observed every twelve hours, such as polar-orbit satellite data have a smaller sampling error. However, if the variation is not symmetrical, the daily-mean data might have a large sampling error as Case-B in Figure 2. In the latter case, we can expect that we reduce the sampling error by increasing the number of a sample during a day or averaging the samples selectively.

Figure 3 shows the root mean square (RMS) error between true daily mean data and data obtained by averaging data sampled every twelve hours. In this figure, a horizontal coordinate indicates sampling time. For example, 00(12) indicates the sampling at midnight and noon. True daily mean data are defined as a value estimated by averaging hourly data. In this figure, we can see the errors of these averaged data depend on the sampling time. The error is the minimum for data sampled at 5 a.m. and 5 p.m. The figure also shows that the error increases toward 00(12) or 11(23). Additionally, this tendency is clear in middle latitudes. Considering about observation time of satellite, we can see that the observation time of DMSP/SSMI F13 gives the smallest sampling error. Next, we calculated the correlation coefficient between the sampling error of 00(12) and that of other data. Figure 4 shows the variation of a correlation coefficient. Shaded parts on this figure indicate the significance level of 99%. In this figure, we found that the error correlation is zero near 05(17). We also find the correlation depends on latitudes. The correlation in low latitudes is weaker than that in middle latitudes. The observation time of Aqua has positive correlation and that of DMSPs has negative correlation. Therefore, it is possible that the sampling error may reduce, if we merge Aqua and DMSP data.

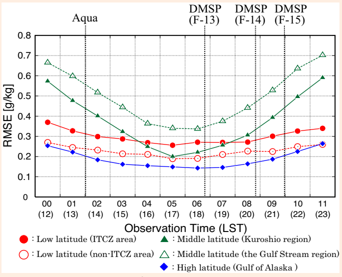

Figure 3. Variation of RMS error between true daily-mean data and data obtained by averaging data sampled every twelve hours.

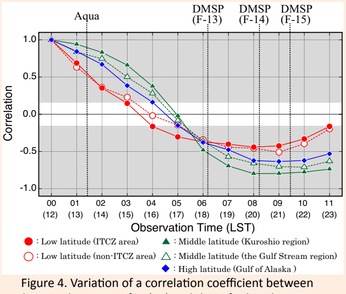

Figure 4. Variation of a correlation coefficient between the sampling error of 00(12) and that of other data.

We investigated how to average the various satellite data is effective for reducing the sampling error. Here, we used only buoy data observed in 2003. Five kinds of multi-satellite combination are examined in this study (see Table 3). In the results shown by Figure 5, we can find that the combination of data observed by DMSPs and Aqua remarkably reduces the RMS error. Figure 4 suggests this result is caused by the inverse relationship between data of DMSPs and Aqua. On the other hand, because DMSPs have similar characteristics with each other, combination of the data is inefficient to reduce the sampling error. Additionally, combination of data observed by TRMM and other satellites is also inefficient to reduce the sampling error, because the observation time of TRMM is different every day.

Table 3. Combination of satellite in simulation.

Satellite	DMSP F-13	DMSP F-14	DMSP F-15	Aqua	TRMM
Observation Time	06, 18	08, 20	09, 21	01, 13	random
SIM-1	O	O	O	X	X
SIM-2	O	O	O	O	X
SIM-3	O	O	O	X	O
SIM-4	X	X	X	O	O
SIM-5	O	O	O	O	O
DMSP F-13	O	X	X	X	X
DMSP F-14	X	O	X	X	X
DMSP F-15	X	X	O	X	X
Aqua	X	X	X	O	X
TRMM	X	X	X	X	O

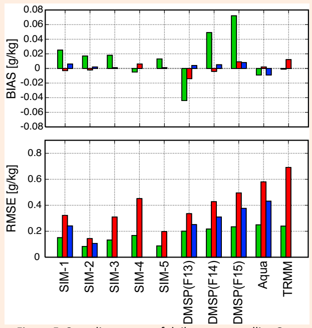

Figure 5. Sampling errors of daily-mean satellite Qa data reproduced by buoy data. Green : low latitude, Red: middle latitude, Blue : High latitude.

(2) Construction of Multi-satellite Qa data

We employed algorithm by Tomita (private communication), Kubota and Hihara (2008) and Iwasaki and Kubota (2011) to estimate the Qa from brightness temperatures observed by DMSP/SSMI, Aqua/AMSR-E and TRMM/TMI, respectively. These algorithms are expressed by linear regression formula.

Additionally, we used the constraint by Schulz et al. (1993) and Schlüssel and Albert (2001) to remove brightness temperature data contaminated by rain fall or cloud liquid water. The former constraint (Schulz et al., 1993) is applied to SSM/I and AMSR-E data, while the latter constraint (Schlüssel and Albert, 2001) is applied to TMI data.

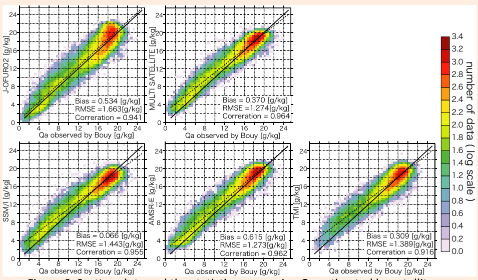

Figure 6. Scatter plots and the statistics comparing Qa estimated by satellite data with Qa observed by buoy

We constructed the global Qa product by merging DMSP/SSMI, Aqua/AMSR-E and TRMM/TMI Qa data. Spatial and temporal resolutions of this product is 1.0 deg. × 1.0 deg. and daily, respectively. We calculated Qa data using a simple average with these three satellite products.

We validate the accuracy of the present product by comparing the product with buoy data. We present the results of validation in Figure 6. Figure 6 shows the scatter plots and statistics. The number of data used in this validation was 41902 except for TRMM/TMI. Because TRMM/TMI doesn't observe in high latitude area, the number of data for TRMM/TMI was 32309. We realize that the Qa data provided by J-OFURO2 has larger scatter than the other Qa data when the value of Qa observed by buoy have over 16 g/kg. On the other hand, as the value of Qa observed by buoy gets smaller, the Qa data calculated in this study tends to overestimate. As compared with the Qa data provided in J-OFURO2, we can see the present product gives the less RMS error. The statistics in all latitudes are shown in Table 4. The RMS error of multi-satellite Qa data was the smallest in low and middle latitudes. This result suggests the reduction of a sampling error. However, in high latitudes, it is not the case.

Table 4. Accuracy of Qa estimated by satellite data every latitudes.

Product	Algorithm	Low lat. (15°S－15°N) Bias[g/kg]	Low lat. RMSE[g/kg]	Low lat. Corr.	Middle lat. (40°N - 15°S ,15°N－40°N) Bias[g/kg]	Middle lat. RMSE[g/kg]	Middle lat. Corr.	High lat. (40°N－60°N) Bias[g/kg]	High lat. RMSE[g/kg]	High lat. Corr.
J-OFURO2	Schlüssel et al. (1995)	0.530	1.615	0.721	0.794	1.826	0.925	0.127	1.535	0.923
MULTI SATELLITE		0.082	1.034	0.810	0.915	1.548	0.950	1.221	1.325	0.931
SSM/I	Tomita algorithm (private note)	-0.359	1.098	0.781	0.731	1.639	0.942	1.507	1.521	0.914
AMSR-E	Kubota and Hihara (2008)	0.478	1.107	0.793	1.098	1.645	0.940	0.618	1.215	0.939
TMI	Iwasaki and Kubota (2011)	0.172	1.215	0.763	0.720	1.750	0.932			
Deta of Number		37036			12425			6756		

(3) Validation of accuracy of LHF estimated from multi-satellite Qa

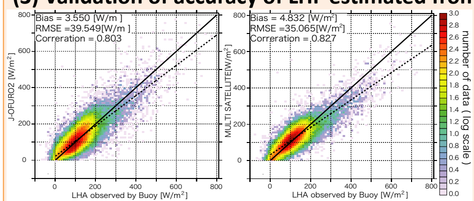

Figure 7. Scatter plots and the statistics comparing the LHF estimated by satellite data with the LHF observed by buoy.

To estimate the LHF, we used multi-satellite Qa data that calculated from three kinds of sensor, and the other physical quantities employed by J-OFURO2. Hereafter, we call this LHF data as MS-LHF. We compared MS-LHF and LHF provided by J-OFURO2 with LHF observed by buoy. The scatterplots with statistics are shown in Figure 7. As the value of LHF observed by buoys increases, MS-LHF tends to underestimate. The RMS error of MS-LHF is smaller approximately 4.5 [W/m2] than that of J-OFURO2. We show results of validation in three areas in Table 5. MS-LHF gives a small RMS error and high correlation in all latitudes compared with those of J-OFURO2 LHF. However, the bias of MS-LHF is bigger in low and middle latitudes.

Table 5. Accuracy of the LHF estimated by satellite data every latitudes.

Product	Low lat. (15°S－15°N) Bias[W/m²]	Low lat. RMSE[W/m2]	Low lat. Corr.	Middle lat. (40°N - 15°S ,15°N－40°N) Bias[W/m2]	Middle lat. RMSE[W/m2]	Middle lat. Corr.	High lat. (40°N－60°N) Bias[W/m2]	High lat. RMSE[W/m2]	High lat. Corr.
J-OFURO2	4.254	34.287	0.723	-5.212	53.434	0.861	20.222	38.073	0.812
MULTI SATELLITE	10.915	28.403	0.745	-9.793	48.489	0.887	-16.114	31.912	0.855
Deta of Number	50036			13599			5034		

4. Conclusion

Previous studies (e. g. Iwasaki et al., 2010) pointed out that highly accurate Qa is important to accurately estimate LHF over the ocean. Thus, we constructed the highly accurate Qa product using multi-satellite data.

First, we examined the error included in daily-mean data calculated by averaging data observed every twelve hours using five kinds of buoy data. For each buoy data, the error is the minimum for data sampled at 5 a.m. and 5 p.m. Additionally, we showed that it is possible to reduce the sampling error by merging the data observed by Aqua/AMSR-E and DMSP/SSMI. On the other hand, the combination of TRMM and other data was not so efficient to reduce the sampling error.

In this study, we constructed the global Qa product by merging DMSP/SSMI, Aqua/AMSR-E and TRMM/TMI. Comparing with the Qa data provided by J-OFURO2, we can see the present Qa product gives a smaller error in all latitudes. Also, the accuracy of the present Qa product is higher than that of single-satellite products in low and middle latitudes. The results suggest the usefulness of multi-satellite product in order to reduce the sampling error.

Acknowledgements

This research was partly funded by the Japan Aerospace Exploration Agency. The buoy data used in this research were provided from National Data Buoy Center and Pacific Marine Environmental Laboratory.

Please freely take one copy

References

Iwasaki S., and M. Kubota, 2011. Development of an algorithm for estimation of air specific humidity using TMI data. *Int. J. Remote Sens.*, in press.
Iwasaki, S., M. Kubota, and H. Tomita, 2010. Evaluation of bulk method for satellite-derived latent heat flux. *J. Geophys. Res.*, 115, C07007.
Kubota, M., and T. Hihara, 2008. Retrieval of surface air specific humidity over the ocean using AMSR-E measurements. *Sensors*, 8, pp. 8016-8026.
Kubota, M., and H. Tomita, 2007. Present state of the J-OFURO air-sea interaction data product. *FLUXNEWS*, 4, pp. 13-15 .
Schulz, J., P. Schüssel, and H. Grassl, 1993. Water vapor in the atmospheric boundary layer over oceans from SSM/I measurements. *Int. J. Remote Sens.*, 14 (15), pp. 2773-2789.
Schüssel P., and A. Albert, 2001. Latent heat flux at the sea surface retrieved from combined TMI and VIRS measurements of TRMM. *Int. J. Remote Sens.*, 22 (10), pp. 1975-1998.